QUDIT ISOTOPY

ARTHUR JAFFE, ZHENGWEI LIU, AND ALEX WOZNIAKOWSKI

Harvard University, Cambridge, MA 02138, USA

February 23, 2016

Abstract. We explore a general diagrammatic framework to understand qudits and their braiding, especially in its relation to entanglement. This involves understanding the role of isotopy in interpreting diagrams that implement entangling gates as well as some standard quantum information protocols. We give qudit Pauli operators X, Y, Z and comment on their structure, both from an algebraic and from a diagrammatic point of view. We explain alternative models for diagrammatic interpretations of qudits and their transformation. Our approach rests on algebraic and topological relations discovered in the study of planar para algebras. In summary, this work provides bridges between the new theory of planar para algebras and quantum information, especially in questions involving entanglement.

1. Introduction

In this paper we give various diagrammatic models of qudits. In our first model, we represent one qudit as a string; in the second (two-string) model it becomes a cap; in a third (four-string) model it is represented by a pair of caps. The particles in each of these models may be parafermion Majoranas, parafermions, or bosons. In the four string model our qudits are bosons that arise as particle-anti-particle pairs.

It is the robust nature of these diagrams, which illustrate properties of states and of operators, that fascinates us. Our general approach is an application of the mathematical framework of *planar para algebras*, that we introduced in [15]. In that paper we elaborate on the general topological properties of the models that we only sketch here.

The main goal of our present work is to provide a link between the new theory of planar para algebras and quantum information. We give a solution to the Yang-Baxter equation that represents a braid. In the

first two models, the braiding of qudits describes qudit entanglement. We also use braiding of qudits to obtain the entanglement distribution protocol, the entanglement-swapping protocol and the entanglement-relay protocol.

We illustrate in Figure 1 the use of a braid to simulate the entanglement provided by the conjunction of a Hadamard and CNOT gate. We construct a similar maximally entangling qudit-braid.

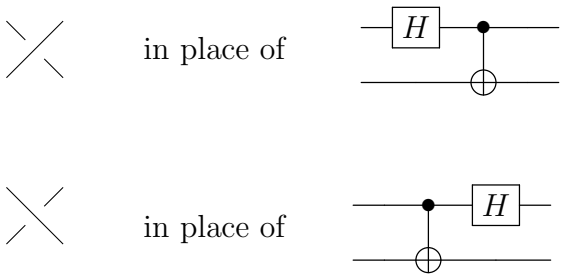

FIGURE 1. Entangling, unitary solution of the Yang-Baxter equation on the left, and entangling quantum circuit on the right.

We use braids such as in Figure 1, but generalized to include particle excitations illustrated in Figure 2. Here the particle with charge k is represented by the label k. As a consequence of the Brylinskis' remarkable criterion, one can employ this braid to obtain a partial topological quantum computer for parafermion Majoranas and parafermions.[1]

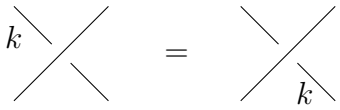

FIGURE 2. Qudit-braid relation.

The *qudit-braid* relation illustrated in Figure 2 shows how a particle moves under the braid crossing. This identity allows us to use topological isotopy in three-dimensional space. This technique was used before in planar algebras, but it is new in the context of braids with particle excitations.

We explain our notation in §2, including the interpretation of the structure of states in terms of diagrams, as well as the interpretation of the trace and partial trace–which enter the process of measurement.

[1]This criterion is Theorem 4.1 of [6]. The preprint and published versions have different organization, and we refer to the numbering in the latter. See also [5].

In §3 we introduce braids that involves particle excitations. There we explain the qudit-braid relation.

In §4 we focus on two different versions of qudit Pauli X, Y, Z matrices, which are useful for interpreting protocols. The diagrammatic presentation of these matrices makes clear the way X, Y, Z are built from qudits, and how one can translate the qudit representation into formulas. In particular, in our four-string model one sees from the diagrams how and why the matrices X, Y, Z act on the charge-zero (gauge-invariant) subspace of a space of qudits.

In §5 we give some applications of the diagrammatic method to understanding entanglement protocols. We address the entanglement-distribution protocol and the entanglement-swapping protocol. We go into one application in detail, in which we realize a quantum circuit using the one-string model (that we employ throughout the bulk of the paper). This model illustrates how we take advantage of *topological isotopy*—a property central to the structure of planar para algebras.

In §6.1–§6.4 we contrast our one-string, two-string, and four-string models. (The four-string model is especially adaptable to certain situations with redundant degrees of freedom, including models for X, Y, Z. Here charge neutrality of qudits as particle-anti-particle pairs plays a natural role.)

In §6.5 we discuss some further applications. In particular we show how our four-string model easily describes controlled gates, that have been studied algebraically in a recent paper of Hutter and Loss [13].

In §7 we define an *entanglement-relay* protocol to implement long-distance entanglement. This protocol allows one to transfer entanglement in a non-local fashion to distant objects.

2. Notation

2.1. **The Parafermion Algebra.** The *parafermion algebra* is a $*$-algebra with unitary generators c_j, which satisfy

$$c_j^d = 1 \quad \text{and} \quad c_j c_k = q\, c_k c_j \quad \text{for } 1 \leqslant j < k \leqslant m. \tag{1}$$

Here $q \equiv e^{\frac{2\pi i}{d}}$, $i \equiv \sqrt{-1}$, and d is the order of the parafermion. Consequently $c_j^* = c_j^{-1} = c_j^{d-1}$ where * denotes the adjoint. Majorana fermions arise for $d = 2$. This is an example of a planar para algebra, for which the general theory provides diagrammatic representations: for elements of this algebra, and for the representation of its action on Hilbert space.

2.2. **Diagrammatic Representation.** We introduce diagrams to represent elements of our algebra or qudits. The diagrams multiply from

bottom to top[2]. Also, tensor products multiply from left to right. We represent the horizontal multiplication XY and the tensor product $X \otimes Y$ by

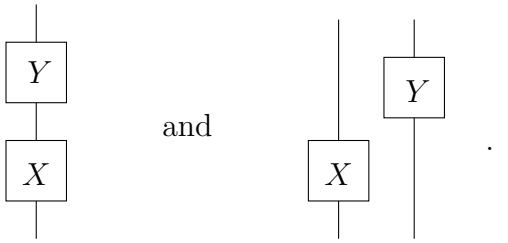

We represent a generator c_j in the j^{th} tensor factor as

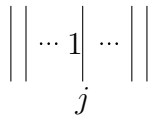

The power c_j^α of c_j arises from replacing the label "1" by the label "α." Additionally,

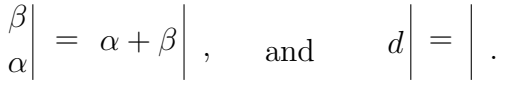

The parafermion relation (1) becomes

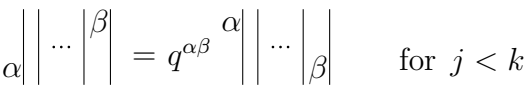

(2)

where the strings between j and k contain no excitations. We call $q^{\alpha\beta}$ the twisting scalar.

Let ζ be a square root of q, with the property $\zeta^{d^2} = 1$. We remark that the diagrammatic interpretation given in [15] of the twisted tensor product $X \circ Y = \zeta^{|X||Y|} XY$ introduced in [16, 14], interpolates between the left and right side of the parafermion relation (2). We write the labels on the same vertical height. Then

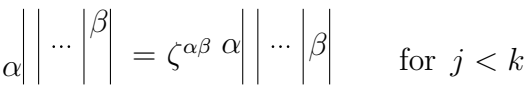

(3)

The diagram called a *cap* is not an element of the parafermion algebra. Rather it is a vector that provides one qudit. We transport the qudit label from left to right on the cap, producing a phase ζ, which

[2]This follows standard conventions for braids, while the standard convention for circuits is multiplication from left to right.

can be interpreted as a Fourier transform relation, see [15]. The cap has the form

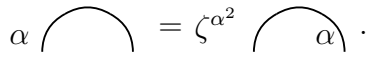

We represent the adjoint * diagrammatically as

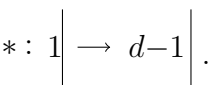

(4)

More generally, the adjoint * of a product comes from its vertical reflection,

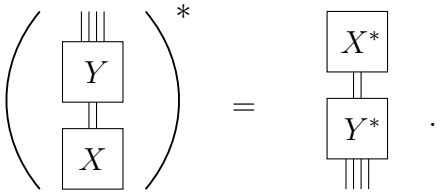

The *cup* diagram is related to the cap above, and it also satisfies a parafermion relation. We obtain the cup from the cap by the adjoint, followed by the substitution $\alpha \to -\alpha$. Thus

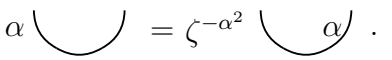

Taken together, the cap and cup correspond to the Dirac braket. This representation will be used in our two-string and four-string models of §6.

2.3. **Trace.** The normalized trace $\mathrm{tr}(\cdot)$ is represented diagrammatically as

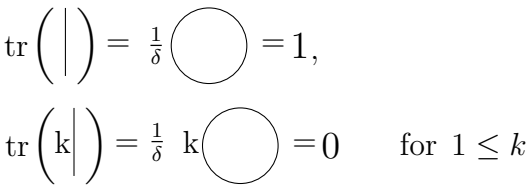

Here $\delta = \sqrt{d}$ represents the circle diagram constant,

2.4. **Inner Product.** The standard, or computational, basis of the $\mathbb{Z}_d$ graded Hilbert space $\mathcal{H}_d(m)$ is $|i_1 i_2 \cdots i_m\rangle \equiv |i_1\rangle \otimes |i_2\rangle \otimes \cdots \otimes |i_m\rangle$, for $0 \leqslant i_1, i_2, \ldots, i_m \leqslant d-1$. This vector is graded by $\sum_{k=1}^{m} i_k \mod \mathrm{d}$. In

our one-string model in §6, we represent the vector $|i_1 i_2 \cdots i_m\rangle$ by

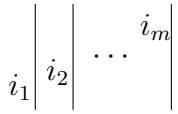

For $x, y \in \mathcal{H}_d(m)$, we represent the inner product $\langle x|y\rangle$ by

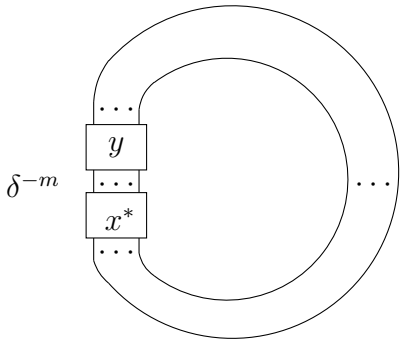

2.5. **Partial Trace.** Planar parafermion algebras are half-braided, allowing a partial trace to be defined. The partial trace $\mathrm{tr}^{j_1,j_2,\cdots,j_k}(\cdot)$ for $1 \le j_1, j_2, \cdots, j_k \le m$ is represented diagrammatically as

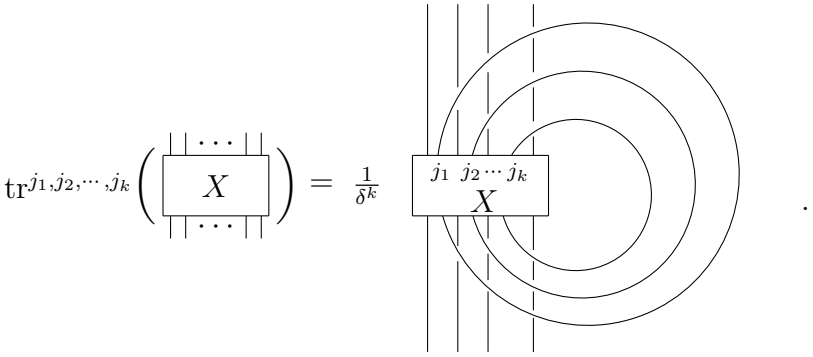

On the right hand side the $j_1, j_2, \cdots, j_k$ strings are closed to form caps. The nonclosed strings always move under the caps. Moreover, the strings are closed clockwise from top to bottom. The spherical condition allows strings to be closed counterclockwise from top to bottom. See §2.2 of [15] for details and the definition of the spherical condition.

2.6. **Measurement.** We use the meter in Figure 3 to perform a measurement of the strings $j_1, j_2, \cdots, j_k$, represented diagramamtically in Figure 4. The result of the measurement is represented in Figure 5. The meter designates that the $j_1, j_2, \cdots, j_k$ strings are to be closed from top to bottom to form caps. We proceed by removing the meter from

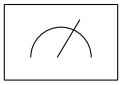

FIGURE 3. Meter.

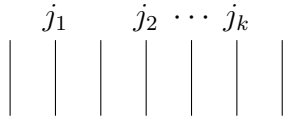

FIGURE 4. Strings to be measured, $j_1, j_2, \cdots, j_k$.

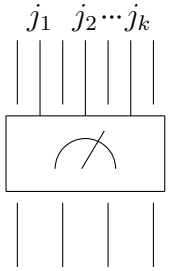

FIGURE 5. Measurement: unmeasured strings pass underneath the meter.

the diagram and closing the $j_1, j_2, \cdots, j_k$ strings, as discussed above for the partial trace.

Let us illustrate a measurement for parafermions of order d. Consider three parafermions in the computational basis

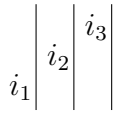

.

Suppose we want to measure the first two tensor factors. We place the meter under the first two strings as illustrated below,

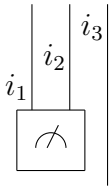

.

The meter under the first two strings designates that those strings are closed to form caps. We obtain

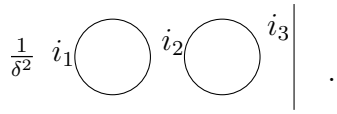

As the circle diagram has value δ, the measurement of an unconnected string with no excitation is normalized to give the value 1.

3. Braids and Entanglement

3.1. **Background.** The topological approach to quantum computation became important with Kitaev's 1997 paper proposing an anyon computer—work that only appeared some five years later in print [20]. In §6 on the arXiv, he described the braiding and fusing of anyonic excitations in a fault-tolerant way. Freedman, Kitaev, Larsen, and Wang explored braiding further [10], motivated by the pioneering work of Jones, Atiyah, and Witten on knots and topological field theory [17, 2, 26].[3] Kauffman and Lomonaco remarked that the braid diagram describes maximal entanglement [19].

3.2. **The Braid.** For fermions and parafermions the parafermionic Fock space $\mathcal{H}_d(m)$ is isomorphic to the m-qudit space $\mathbb{C}^{d^m}$, where d denotes the parafermion order and m is the number of modes. The choice of $d = 2$ is the standard Fock space for m fermionic modes, which is isomorphic to the m-qubit space [22].

The notion of fermionic entanglement for pure states was analyzed in [23, 24, 3], whereby product states are those that one can write as a tensor product in the Fock representation. This definition of entanglement naturally generalizes to the case of parafermionic pure states. We refer to this generalization as *parafermionic entanglement*.

The unitary braid operator[4] in Figure 6 canonically generates maximal fermionic and parafermionic entanglement for arbitrary finite dimensions. See §8 of [15] for details and the definition of the braid

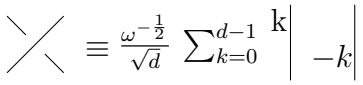

Figure 6. Braid diagram for entanglement.

[3]Diagrammatic notation in quantum information theory originated in the quantum circuit model of Deutsch [8], although without the consideration of topology.

[4]These braids can be "Baxterized" in the sense of Jones [18]. They are the limits of solutions to the Yang-Baxter equation in statistical physics [27, 4], and have actually been introduced earlier in [9]. Such kinds of braid statistics in field theory and quantum Hall systems were considered extensively by Fröhlich, see [11, 12].

where $\omega = \frac{1}{\sqrt{d}} \sum_{j=0}^{d-1} \zeta^{j^2}$ is a phase. (Recall $\zeta^2 = q$, and $q^d = \zeta^{d^2} = 1$.) The braid has the special property that qudit excitations can move under the braid crossing as illustrated in Figure 2.

Since the braid is unitary, its adjoint equals the inverse braid

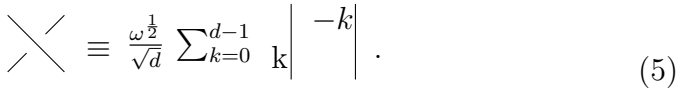

(5)

This inverse disentangles fermionic and parafermionic states of arbitrary finite dimension in a canonical way.

In the following example we illustrate maximal entanglement for the fermionic case $d = 2$. Consider the two-qubit space

$$\mathbb{C}^4 = \mathrm{Span}_{\mathbb{C}}\left\{ \left|\,\right|, \left|\,1\right|, 1\left|\,\right|, 1\left|\,-1\right| \right\},$$

in which the braid acts on the basis by

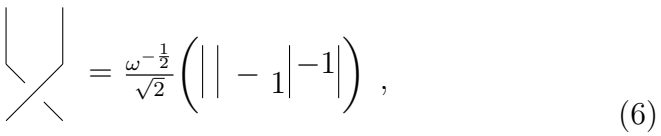

(6)

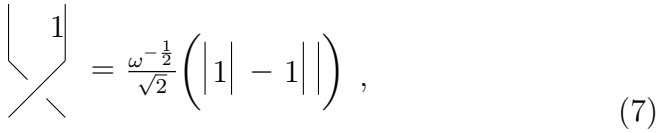

(7)

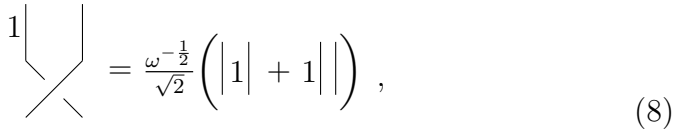

(8)

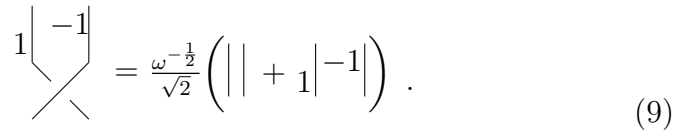

(9)

In quantum computation the braid is "imprimitive" in the sense of the Brylinskis, since it is *entangling*. This result yields a partial topological quantum computer for fermions and parafermions. Additionally, the braid may be applied to construct several quantum information protocols diagrammatically, which consume entanglement as a resource.

In Figure 7 we illustrate the braid b_i on the ith and $i+1$th strings.

$b_i =$ 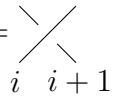

FIGURE 7. Braid between Adjacent Strings.

4. Qudit Pauli X, Y, Z Matrices

One can find qudit, Pauli X, Y, Z matrices that satisfy the relations

$$X^d = Y^d = Z^d = 1 \,, \tag{10}$$

$$YX = q\,XY \,, \quad ZY = q\,YZ \,, \quad \text{and} \quad XZ = q\,ZX \,. \tag{11}$$

Here $q = e^{\frac{2\pi i}{d}}$. These matrices must also satisfy a second set of relations defined in terms of a square root $\zeta = q^{\frac{1}{2}}$ for which $\zeta^{d^2} = 1$, namely

$$XYZ = YZX = ZXY = \zeta^{-1} \,. \tag{12}$$

In §4 of [15] we give two different solutions $\widehat{X}, \widehat{Y}, \widehat{Z}$ for X, Y, Z. Each solution is a quadratic function of four qudit generators c_1, c_2, c_3, c_4 of the parafermion algebra.

4.1. **Solution I.** In §5 of [15] we give a diagrammatic interpretation for these operators. Our first solution has the form

$$\widehat{X} = \zeta\, c_1^{-1} c_4 \,, \quad \widehat{Y} = \zeta\, c_2 c_4^{-1} \,, \quad \widehat{Z} = \zeta\, c_3^{-1} c_4 \,. \tag{13}$$

These matrices satisfy relations (10)–(11), but they do not identically satisfy (12) on the entire Hilbert space.

As explained in [15], the product $\widehat{X}\widehat{Y}\widehat{Z}$ has the form

$$\widehat{X}\widehat{Y}\widehat{Z} = \widehat{Y}\widehat{Z}\widehat{X} = \widehat{Z}\widehat{X}\widehat{Y} = \zeta^{-1}\gamma \,, \quad \text{where} \quad \gamma = q c_1^{-1} c_2 c_3^{-1} c_4 = e^{iQ} \,, \tag{14}$$

defining the self-adjoint charge operator Q mod $\mathbb{Z}_d$. Since $\widehat{X}$, $\widehat{Y}$, $\widehat{Z}$ are zero-graded, each operator acts on the eigenspaces of γ. One achieves the missing relations (12) by restricting to the charge-zero subspace for which $\gamma = +1$.

4.2. **Solution II.** Our second solution is

$$\widehat{X} = \zeta\, c_1^{-1} c_2 \,, \quad \widehat{Y} = \zeta\, c_1 c_3^{-1} \,, \quad \widehat{Z} = \zeta\, c_1^{-1} c_4 \,. \tag{15}$$

These matrices $\widehat{X}$, $\widehat{Y}$, $\widehat{Z}$ also satisfy the relations (10)–(11) and (14). So they satisfy (12) on the same eigenspace $\gamma = +1$. One can perform this construction at each one of various sites labelled by a subscript j, giving rise to a representation of operators $\widehat{X}_j, \widehat{Y}_j, \widehat{Z}_j$ at each site, and that mutually commute at different sites.

Diagrammatically our two solutions (13) and (15) lead to very different looking models, which in §6 we call four-string models (each string representing a qudit) of Type I and Type II. In the related paper [15], we give details and develop these results in a more general context.

4.3. **Comparison with Kitaev's $d = 2$ construction.** Solution I, given in §4.1, is related to the construction of Kitaev for $d = 2$. However our Solution I is different in a subtle way from Kitaev's construction. Equation (11) of [21] gives the $d = 2$ representation that one commonly uses in condensed-matter physics, in which

$$\widehat{X} = i\, c_1 c_4 \ , \quad \widehat{Y} = i\, c_2 c_4 \ , \quad \widehat{Z} = i\, c_3 c_4 \ ,$$

and one has

$$\widehat{X}\widehat{Y}\widehat{Z} = \widehat{Y}\widehat{Z}\widehat{X} = \widehat{Z}\widehat{X}\widehat{Y} = ic_1c_2c_3c_4 \ .$$

One takes

$$\widehat{X}\widehat{Y}\widehat{Z} = \widehat{Y}\widehat{Z}\widehat{X} = \widehat{Z}\widehat{X}\widehat{Y} = i \ ,$$

on the subspace for which $c_1c_2c_3c_4 = 1$.

We can recover this solution of Kitaev from our formulas, by taking $d = 2$, $\zeta = i$, and $\gamma = -1$ (rather than $\gamma = +1$ as we require). Likewise for general d, one could take

$$\widehat{X}\widehat{Y}\widehat{Z} = \widehat{Y}\widehat{Z}\widehat{X} = \widehat{Z}\widehat{X}\widehat{Y} = \zeta^{-1}q^k \ ,$$

on the subspace graded by k mod d, where $\gamma = q^k$.

In our four-string model described in §6.4, we represent a qudit by a charge-zero, particle-anti-particle pair. The neutral total charge means that $\gamma = +1$. For this reason we find our choice natural. And with this basis, the Pauli X, Y, Z act as $d \times d$ matrices in a natural way.

In Kitaev's model $\gamma = -1$, so qudits are not neutral. Hence one loses the particle-anti-particle interpretation of qudits that we exploit in our diagrams.

5. Protocols

5.1. **Entanglement Distribution Protocol.** We apply the braid to construct the entanglement distribution protocol. Consider the computational basis for two parafermions of order d,

$$\left| i_1 \right| \left| i_2 \right| \qquad \text{for} \quad 0 \le i_1, i_2 \le d-1 .$$

We act with the braid of Figure 6 to generate maximal entanglement, namely

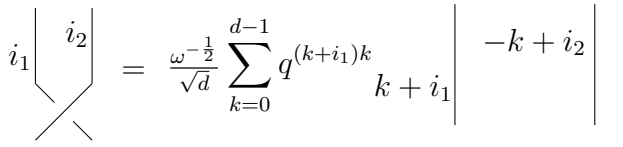

(16)

The special case of fermions was shown in (6)–(9). The remaining step of the protocol involves distribution of the entanglement through a noiseless quantum channel [25]. Such a channel leaves (16) invariant. Physically the distribution is performed by a variety of methods [1, 7].

5.2. **Entanglement-Swapping Protocol.** We can also apply the braid to construct the entanglement-swapping protocol. This protocol inputs four disentangled fermionic or parafermionic states, and maximally entangles two of the states without trivially braiding them. Physically these entangled states do not need to share any common past [28].

Consider the diagram below, which entangles the first and second strings, and it entangles the third and fourth strings. Then, it disentangles the second and third strings with the inverse braid:

(17)

We proceed by placing the meter, introduced in §2.6, under the second and third strings of (17), as illustrated below

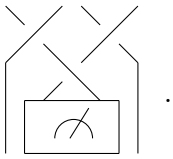

(18)

We claim that (18) acts by maximally entangling the leftmost and rightmost input states as desired. Here we use the relations in §8 of [15].

We remove the meter in (18), closing the second and third strings to form caps as illustrated below

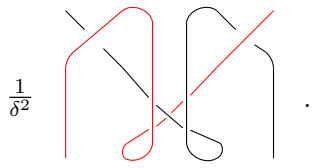

(19)

Isotopy is a property of parafermion planar algebra. This topological notion simplifies the computation of (19) and reduces it to a scalar multiple of the braid. It permits us to move the strings in three-dimensional space. We note that the red string under the Reidemeister moves becomes the braid's over crossing. We use the second Reidemeister move on (19) to obtain

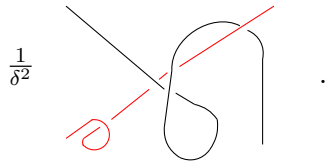

Application of the second and third Reidemeister moves simplifies the diagram above to

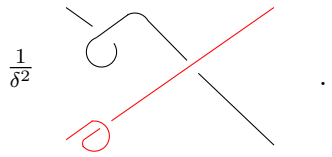

The braid and its inverse in the last diagram above have opposite coefficients by the first Reidemeister move, reducing the diagram to

Therefore, the entanglement-swapping diagram in (18) maximally entangles the leftmost and rightmost input states without trivially braiding them. The end result is shown in Figure 8, where we suppress the factor δ^{-2}. Note that in contrast to the topological moves that we have used, an algebraic approach based on expanding the braid into a sum of the basis elements leads to a complicated computation for Figure 8.

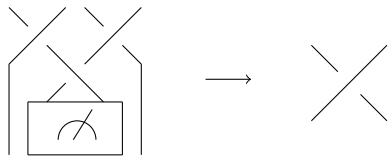

FIGURE 8. Entanglement-swapping diagram.

The entanglement-swapping protocol with braids holds for arbitrary d. In Figure 9 we illustrate the fermionic case $d = 2$.

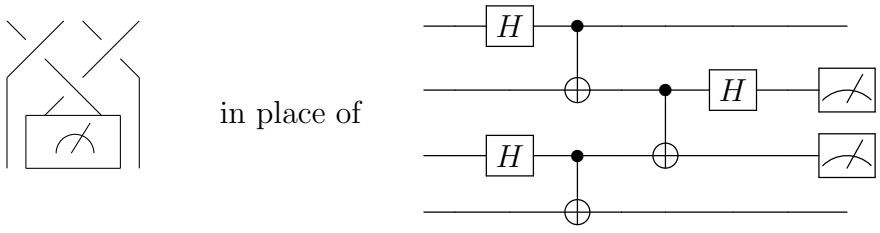

FIGURE 9. Entanglement-swapping with braids on the left, and a quantum circuit on the right.

Remark 5.1. Pictorial representation of other protocols, such as teleportation, superdense coding, and the EPR protocol for quantum key distribution, could be studied by these methods.

6. Different models for quantum information

We contrast one-string, two-string, and four-string models, in order to represent quantum information in terms of diagrams. The qudits are given by Majoranas, parafermions, or bosons, respectively.

6.1. **The One-String Model.** In §2 we realized a qudit by a single labeled string. We replace m qudits, represented algebraically as $|k_1 k_2 \cdots k_m\rangle$, by the diagram

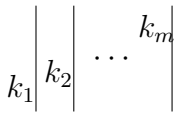

.

Transformations X on m qudits were realized by diagrams with m input points and m output points, and they are represented as

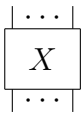

.

The measurement of m qudits is represented by the trace as

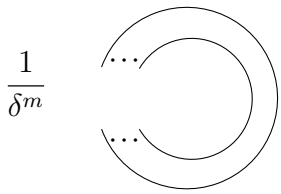

.

We call this representation of quantum information the *one-string model*. In this model the Hilbert space is $\mathbb{Z}_d$ graded. So, the transformations act on different components as the graded tensor product. We note that the diagrams used in the previous sections, such as the braid, are zero graded, or globally gauge invariant. Thus, the twisting scalar $q^{\alpha\beta} = 1$, which reduces the graded tensor product to the usual tensor product.

6.2. **The Type I, Two-String Model.** For the two-string models, each qudit is a parafermion. In the *type I, two-string model*, we realize a qudit by one labeled cap

Here $0 \leq k \leq d-1$. We represent m-qudits by

A transformation on m qudits is represented by a box with $2m$ strings on top and $2m$ strings on the bottom.

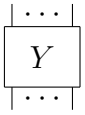

The one-string model can be embedded into the type I two-string model by making the following replacements:

Qudit :

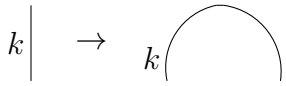

m-Qudits :

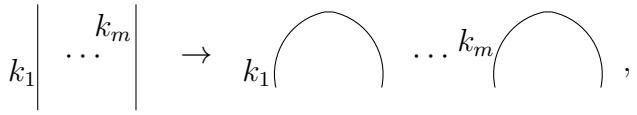

Transformation :

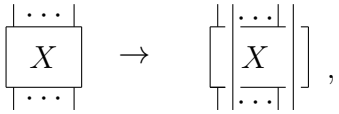

Measurement :

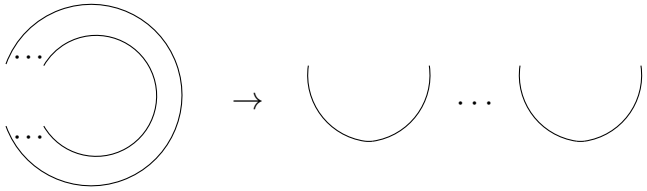

6.3. **The Type II, Two-String Model.** In the type II, two-string model, we represent m-qudits by labeled caps

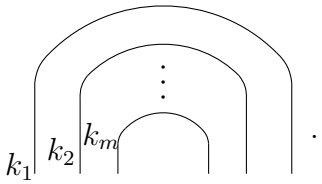

A transformation on m qudits is also represented in this model by a box with $2m$ strings on top and $2m$ strings on the bottom, namely

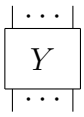

The one-string model can be embedded into the type II two-string model by replacements of a transformation similar to (6.2). The image of the transformation acting on m qudits becomes

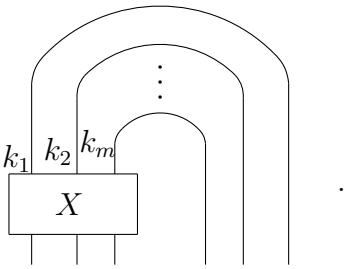

The measurement is represented by

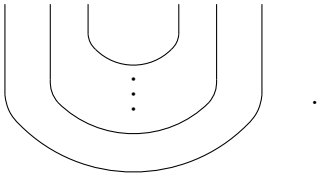

(20)

6.4. **The Four-String Model.** For the four-string model, each qudit is bosonic. In other words a qudit always has particle-antiparticle pairs that yield a total grading zero. For the type I four-string model, we realize a qudit by two labeled caps. We represent m-qudits by the picture:

Here $0 \leq k_i \leq d-1$.

For the type II four-string model, we represent m-qudits by the diagram:

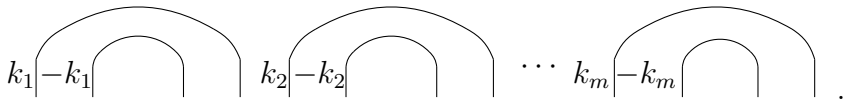

Again $0 \leq k_i \leq d-1$.

A transformation on a single qudit is a zero graded diagram represented by

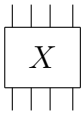

A transformation on m-qudits is a linear sum of tensor products of m single qudit transformations represented by

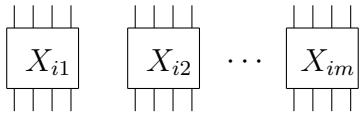

Here X_{ij} is zero graded.

We note that the four-string model is different from the one-string model and the two-string model, where all diagrams with proper inputs and outputs are transformations on qudits. In the four-string model we are interested in diagrams that preserve the subspace spanned by qudits, diagrams given by caps. The following example is not a transformation on 2-qudits:

6.5. **Double Braids as Controlled Gates.** Let us construct some controlled transformations for the type I four-string model. For a transformation A acting on a single qudit, define the controlled transformation C_A on 2-qudit states $|ij\rangle = |i\rangle|j\rangle$ as

$$C_A|ij\rangle = |i\rangle\, A^i|j\rangle\ . \tag{21}$$

We use the matrices X, Y, Z given in (13) for A, to describe the action on a single qudit, giving C_X, C_Y, C_Z.

The double braid S is illustrated in Figure 10. It preserves 2-qudits. Furthermore the double braid is the square of the controlled Z, namely

$$S = C_Z^2\ . \tag{22}$$

The relation (22) has been shown to be true by using algebraic identities [13]. Here we give an elementary proof using diagrams. In fact

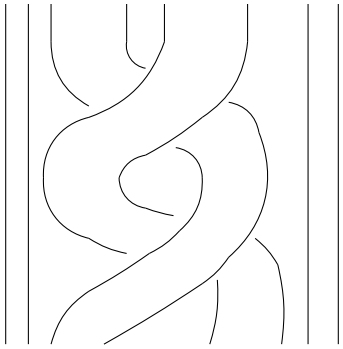

FIGURE 10. The Double Braid.

the proof follows from the qudit-braid relation given in Figure 2. We illustrate our proof with the isotopy in Figure **??**.

One can obtain qudit matrices X, Y from the matrix Z by the conjugation of braids b_i of the i^{th}-string given in Figure 7. As in §5.2.2 of [15], one has:

$$Y = b_2 Z^* b_2^*;$$
$$X = b_1 b_2 Z b_2^* b_1^*.$$

Thus

$$C_Y^2 = b_6 S^* b_6^*;$$
$$C_X^2 = b_5 b_6 S b_6^* b_5^*.$$

Correspondingly, both C_Y^2 and C_X^2 also preserve the subspace spanned by qudits and both are represented by braided diagrams.

7. Entanglement-Relay Protocol

One can extend our earlier discussion in §5.2 in order to create an entanglement-relay network to produce and share *long-distance entanglement*. We now show how to enable entanglement that is non-local. Such entanglement might be across a device, allowing for non-local entangling gates, or it might involve a network of distributed devices.

Let us describe the situation in detail in the case that Alice wants to entangle her qudit with the qudit of Bob, utilizing the aid of three intermediate helpers, H1, H2, and H3, who line up from left to right. The idea is that each person uses a nearest-neighbor for entanglement swapping. Each swap involves one measurement station, which we might call M1, ..., M4. We illustrate this protocol in Figure 12. The resolution of the protocol implements topological isotopy. This produces an

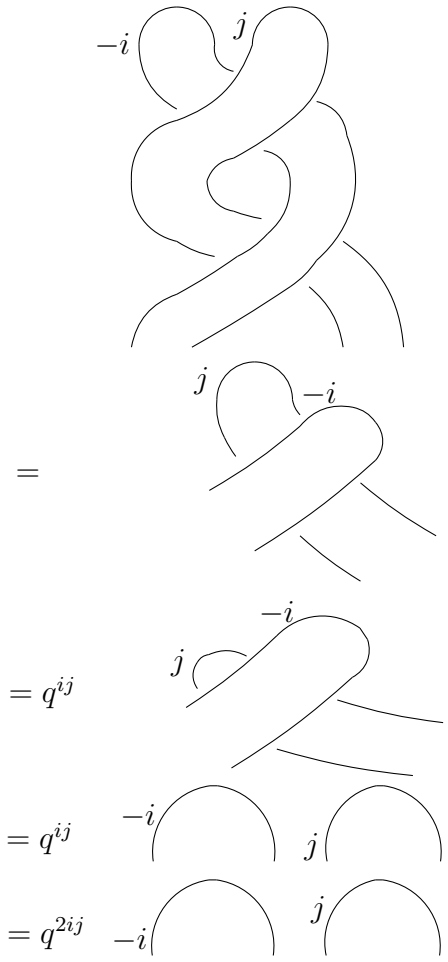

FIGURE 11. Double Braid Relation

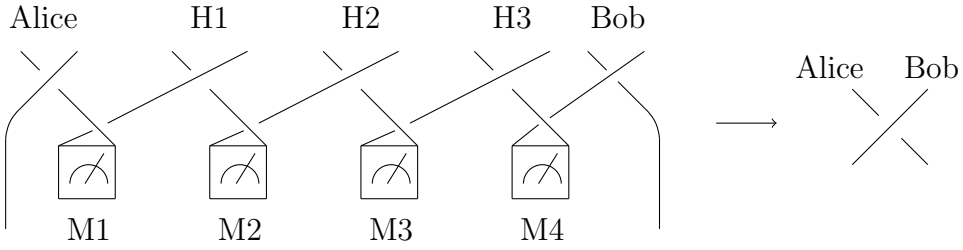

FIGURE 12. Entanglement-Relay with Three Helpers.

overall constant δ^{-8} which we can ignore, as this factor does not affect the entanglement.

The end result is the maximal entanglement of Alice's qudit with the qudit of Bob. It is clear that this situation generalizes for any number $\#H$ of helpers, in which case the constant would be $\delta^{-2(\#H+1)}$.

Acknowledgement

This research was supported in part by a grant from the Templeton Religion Trust. We are also grateful for hospitality at the FIM of the ETH-Zurich, where part of this work was carried out.

References

[1] M. Asperlmeyer, H. R. Böhm, T. Gyatso, T. Jennewein, R. Kaltenbaek, M. Lindenthal, G. Molina-Terriza, A. Poppe, K. Resch, M. Taraba, R. Ursin, P. Walther, and A. Zeilinger, Long-distance free-space distribution of quantum entanglement, *Science* **01**, Vol. 301 Issue 5633, (2003) 621–623, doi:10.1126/science.1085593.

[2] M. F. Atiyah, Topological quantum field theory, Publications Mathématiques de l'IHÉS **68** (1988), 175–186, doi:10.1007/BF02698547.

[3] M. Bañuls, J. I. Cirac, and M. M. Wolf, Entanglement in fermionic systems, *Phys. Rev. A* **76**, (2007) 022311, doi:10.1103/PhysRevA.76.022311.

[4] R. Baxter, Eight-vertex model in lattice statistics and one-dimensional anisotropic Heisenberg chain I, II, III, *Ann. Phys.* **76** (1973), 1–24, 25–47, 48–71, doi:10.1016/0003-4916(73)90439-9.

[5] M. J. Bremner, C. M. Dawson, J. L. Dodd, A. Gilchrist, A. W. Harrow, D. Mortimer, M. A. Nielson, and T. J. Osborne, Practical scheme for quantum computation with any two-qubit entangling gate, *Phys. Rev. A* **89**, (2002) 247902, doi:10.1103/PhysRevLett.89.247902.

[6] J. L. Brylinski and R. Brylinski, Universal quantum gates, in Mathematics of Quantum Computation, G. Chen and R. K. Brylinski, Editors, Chapman & Hall/CRC, Boca Raton, Florida 2002, http://arxiv.org/pdf/quant-ph/0108062v1.pdf.

[7] J. I. Cirac, H. J. Kimble, and H. Mabuchi, Quantum state transfer and entanglement distribution among distant nodes in a quantum network, *Phys. Rev. Lett.* **78** (1997), 3221, doi:10.1103/PhysRevLett.78.3221.

[8] D. Deutsch, Quantum computational networks, *Proceedings of the Royal Society of London. Series A, Mathematical and Physical Sciences*, Vol. 425, No. 1868 (1989), 73–90, doi:10.1098/rspa.1989.0099.

[9] V. Fateev and A. B. Zamolodchikov, Self-dual solutions of the star-triangle relations in $\mathbb{Z}_N$-models, *Physics Letters* **92A** (1982), 37–39, doi:10.1016/0375-9601(82)90736-8.

[10] M. H. Freedman, A. Kitaev, M. J. Larsen, and Z. Wang, Topological quantum computation, *Bulletin of the American Mathematical Society* Volume 40, Number 1, (2002), 31–38, doi:10.1090/S0273-0979-02-00964-3.

[11] J. Fröhlich, New super-selection sectors ("Soliton-States") in two-dimensional Bose quantum field models, *Commun. Math. Phys.* **47** (1976), 269–310, http://projecteuclid.org/download/pdf_1/euclid.cmp/1103899761.

[12] J. Fröhlich, Statistics of fields, the Yang-Baxter equation, and the theory of knots and links, in *Non-Perturbative Quantum Field Theory*, G. 't Hooft et al. (eds.) New York, Plenum Press 1988, doi:10.1007/978-1-4613-0729-7_4.
[13] A. Hutter and D. Loss, Quantum computing with parafermions, (2015), http://arxiv.org/abs/1511.02704.
[14] A. M. Jaffe and B. Janssens, Characterization of reflection positivity, *Commun. Math. Phys.*, to appear, http://arxiv.org/abs/1506.04197.
[15] A. M. Jaffe and Z. Liu, Planar para algebras, reflection positivity, to appear, http://arxiv.org/abs/1602.02662.
[16] A. M. Jaffe and F. L. Pedrocchi, Reflection positivity for parafermions, *Commun. Math. Phys.*, **337** (2015), 455–472, doi:10.1007/s00220-015-2340-x.
[17] V. F. R. Jones, Hecke algebra representations of braid groups and link polynomials, *Ann. of Math* **126** (1987), no. 2, 335–388, doi:10.2307/1971403.
[18] V. F. R. Jones, Baxterization, *Inter. J. Modern Physics A* **6** (1991), no. 12, 2035–2043, doi:10.1007/978-1-4684-9148-7_2.
[19] L. Kauffman and S. Lomonaco Jr., Braiding operators are universal quantum gates, *New J. Phys.* **6** (2004) 134, doi:10.1088/1367-2630/6/1/134.
[20] A. Kitaev, Fault-tolerant quantum computation by anyons, *Ann. Phys.* **303** (2003), 2–30, arXiv:quant-ph/9707021, doi:10.1016/S0003-4916(02)00018-0.
[21] A. Kitaev, Anyons in an exactly solved model and beyond, *Ann. Phys.* **306** (2006) 2–111, doi:10.1016/j.aop.2005.10.005.
[22] M. A. Nielsen, The Fermionic canonical commutation relations and the Jordan-Wigner transform, (2005), http://michaelnielsen.org/blog/archive/notes/fermions_and_jordan_wigner.pdf.
[23] J. Schliemann, D. Loss, A. H. MacDonald, Double-occupancy errors, adiabaticity, and entanglement of spin-qubits in quantum dots, *Phys. Rev. B* **63** (2001), 085311, doi:10.1103/PhysRevB.63.085311.
[24] J. Schliemann, J. Ignacio Cirac, M. Kuś, M. Lewenstein, and D. Loss, Quantum correlations in two-fermion systems, *Phys. Rev. A* **64**, (2001) 022303, doi:10.1103/PhysRevA.64.022303.
[25] M. M. Wilde, Quantum Information Theory, *Cambridge University Press* 2013, 136–176.
[26] E. Witten, Topological quantum field theory, *Comm. Math. Phys.* **117** (1988), no. 3, 353–386, http://projecteuclid.org/download/pdf_1/euclid.cmp/1104161738.
[27] C. N. Yang, Some exact results for the many-body problem in one dimension with repulsive delta-function interaction, *Phys. Rev. Lett.*, **19** (1967), 1312–1314, doi:10.1103/PhysRevLett.19.1312.
[28] M. Zukowski, A. Zeiling, M. A. Horne, and A. K. Ekert, "Event-ready-detectors" Bell experiment via entanglement swapping, *Phys. Rev. Lett.* **71**, (1993) 4287, doi:10.1103/PhysRevLett.71.4287.